Constraint Effects on Cohesive Failures in Low-k Dielectric Thin Films

Ting Y. Tsui, Andrew J. McKerrow, and Joost J. Vlassak
Silicon Technology Development, Texas Instruments Inc, Dallas, TX 75246, U.S.A.
Division of Engineering and Applied Sciences, Harvard University, Cambridge MA 02138

ABSTRACT

One of the most common forms of cohesive failure observed in brittle thin films subjected to a tensile residual stress is channel cracking, a fracture mode in which through-film cracks propagate in the film. The crack growth rate depends on intrinsic film properties, residual stress, the presence of reactive species in the environment, and the precise film stack. In this paper, we investigate the effect of various buffer layers sandwiched between a brittle carbon-doped-silicate (CDS) film and a silicon substrate on channel cracking of the CDS film. The results show that channel cracking is enhanced if the buffer layer is more compliant than the silicon substrate. Crack velocity increases with increasing buffer layer thickness and decreasing buffer layer stiffness. This is caused by a reduction of the constraint imposed by the substrate on the film and a commensurate increase in energy release rate. The degree of constraint is characterized experimentally as a function of buffer layer thickness and stiffness, and compared to the results of a simple shear lag model that was proposed previously.

INTRODUCTION

To reduce device size and power consumption, advanced electronic devices are often made of thin-film composite structures that contain very brittle materials. Films with a residual tensile stress may be subject to delamination or cohesive fracture [1-6]. One common cohesive failure mode is channel cracking, where through-film cracks propagate in the film [6]. The energy

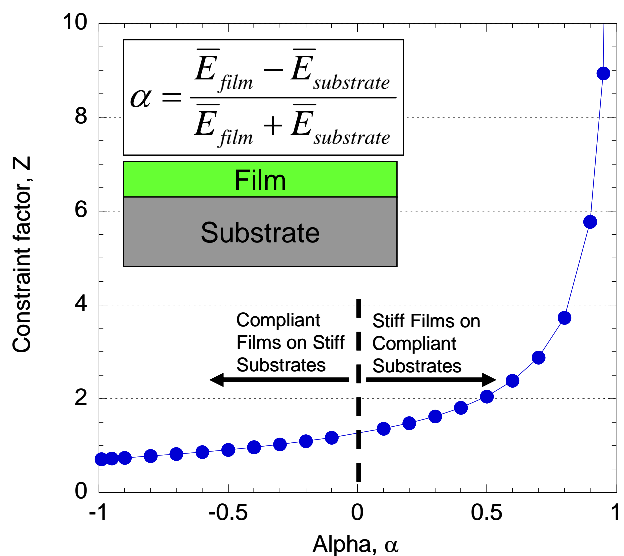

FIG. 1. Plot of the constraint factor (Z) as a function of Dundurs parameters, α and β = α/4 [7].

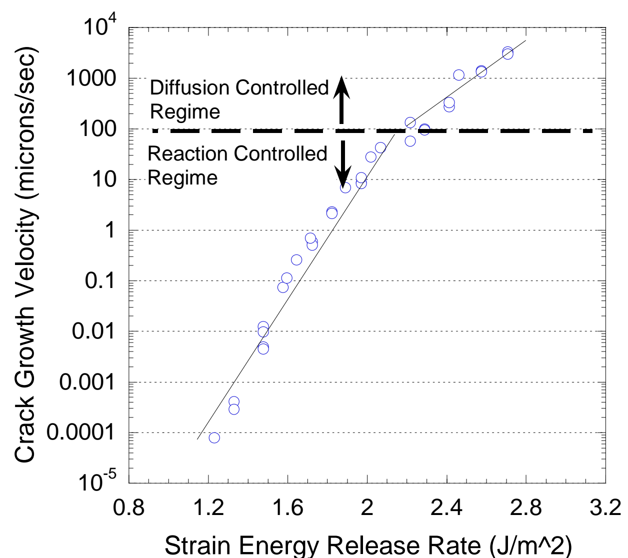

FIG 2. Plot of CDS crack growth rate as a function of energy release rate.

release rate, G, for a channel crack can be calculated using the following equation:

$$G = Z \frac{\pi}{2} \frac{\sigma^2 h}{\bar{E}}, \quad (1)$$

where h, σ, and $\bar{E} = E/(1-\nu^2)$ represent the film thickness, residual stress, and plane-strain elastic modulus, respectively. Z is a constant that depends on the elastic mismatch between film and substrate and on the precise geometry. The effect of elastic mismatch on the energy release rate has been calculated by Beuth [7] for films on half spaces and by Vlassak [5] for films on substrates of finite thickness. The factor Z can be expressed as a function of the plane-strain Dundurs parameters [5, 7-8]

$$\alpha = \frac{\bar{E}_f - \bar{E}_s}{\bar{E}_f + \bar{E}_s}, \qquad \beta = \frac{\mu_f (1-2\nu_s) - \mu_s (1-2\nu_f)}{2\mu_f (1-\nu_s) + 2\mu_s (1-\nu_f)}, \quad (2)$$

where μ represents the shear modulus and ν Poisson's ratio. The subscripts correspond to film (f) or substrate (s) properties. Figure 1 shows a graph of Z calculated by Beuth [7] as a function of α with $\beta = \alpha/4$ for a film on a half space. The figure shows that Z does not vary significantly when α is negative, i.e., for a compliant film on a stiff substrate. If α is greater than zero, however, the film is stiffer than the substrate and Z increases rapidly. This suggests that the driving force for channel cracking is relatively insensitive to the substrate properties when a compliant film is deposited on a stiff substrate. In contrast, the energy release rate changes quickly if the same film is bonded to a substrate that is more compliant than the film.

Even when the driving force for channel cracking is less than the fracture toughness of the film, channel cracking may occur if there is a chemical species in the environment that reacts with the strained bonds at a crack tip. Both experiments and physical models suggest an exponential relationship between crack velocity and energy release rate in the reaction control regime [6-9]:

$$V = V_o \, e^{\left(\frac{Z\pi \sigma^2 h}{4\bar{E}NkT}\right)}, \quad (3)$$

where k is the Boltzmann constant, T the absolute temperature, N the bond density, and V_o a reference velocity. Equation (3) shows that, for a constant film stress, the crack velocity increases exponentially with film thickness, h, and constraint factor Z. Crack velocity is thus a sensitive measure of the effect of the substrate constraint on the energy release rate.

In this article, the constraint effect of buffer layers on channel crack propagation rate is investigated for tensile carbon-doped silicate (CDS) coatings. Samples with underlying films that are either stiffer or more compliant than CDS are investigated. It is demonstrated that the energy release rate and hence channel crack growth depend strongly on the elastic properties and thickness of the under-lying layer.

PROCEDURE

Tensile carbon-doped silicate (CDS) films were deposited using plasma-enhanced chemical vapor deposition (PECVD) near 400°C. Tetra-methylcyclo-tetrasiloxane (TMCTS) was used as

	Elastic modulus (GPa)	Plane-strain modulus (GPa)	Residual stress (MPa)
Si*	163	172	n/a
SiN_x	155	165	-125 ± 5
SiO_2	70	75	-135 ± 5
CDS	8.0	8.5	60 ± 2
Polymer	3.5	3.7	60 ± 2
LD-CDO	3.5	3.7	60 ± 3

* Polycrystalline values calculated from single-crystal elastic constants [11]

Table 1. Material properties of coatings used in this work.

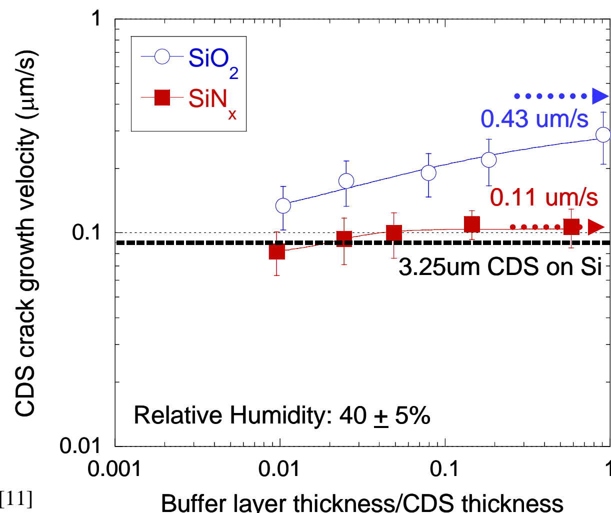

FIG. 3. Plot of CDS crack growth rate as a function of normalized buffer layer thickness.

the silicon and carbon source for the film. The precursor was mixed with oxygen gas in the deposition chamber to form a carbon-doped silicate. To study the substrate constraint effect on channel cracking, thin films with different elastic modulus values were deposited on bare (100) silicon substrates prior to deposition of the CDS films. The under-layers include silicon nitride (SiN_x), tetra-ethoxysilane (TEOS) silicon dioxide (SiO_2), octa-methylcyclo-tetrasiloxane (OMCTS) low-density carbon-doped silicon oxide (LD-CDO), and a poly-aromatic polymer. A summary of the mechanical properties of the CDS and under-layers is given in Table 1 and in reference [3]. All films except the organic polymer were deposited in the temperature range from 350°C to 400°C using PECVD. The polymer films were spin-coated under ambient conditions with a final anneal in forming gas at 400°C for 30 minutes.

Channel crack growth in CDS films was studied in a controlled air environment at a temperature of 21±2°C and a relative humidity in the range of 40 ± 5%. Cracks were induced by scratching samples with a sharp diamond scribe.

RESULTS AND DISCUSSIONS

Figure 2 shows the crack growth velocity for CDS films deposited on bare silicon substrates as a function of energy release rate. Crack growth rate data were collected over a wide range of velocities from 10^{-4} to 10^{3} µm/sec. The figure shows two distinct regimes in the fracture behavior. At low velocities, the crack growth rate increases exponentially with film thickness. This is an indication that fracture of the CDS films in this velocity range is reaction-rate limited [9-10]. At velocities exceeding 100 µm/s, however, transport of the active species to the crack tip becomes important and the slope of the velocity curve is reduced [9-10]. In the following sections, the data in Fig. 2 will be used as a “master curve” to illustrate the effect of underlying layers on the energy release rate and the corresponding channel crack velocity in CDS films.

In order to quantify the effect of underlying layers on crack propagation in CDS, thin films with elastic moduli greater than and smaller than the CDS were used as buffer layers between the silicon substrate and the CDS films. First, the effect of SiN_x and SiO_2 buffer layers will be discussed. Both materials have modulus values greater than CDS, but smaller than silicon.

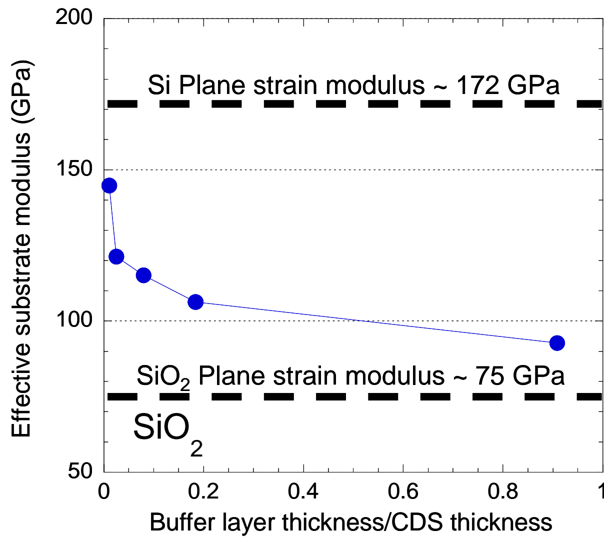

FIG. 4a. Effective substrate modulus of SiO_2 buffer layer sample

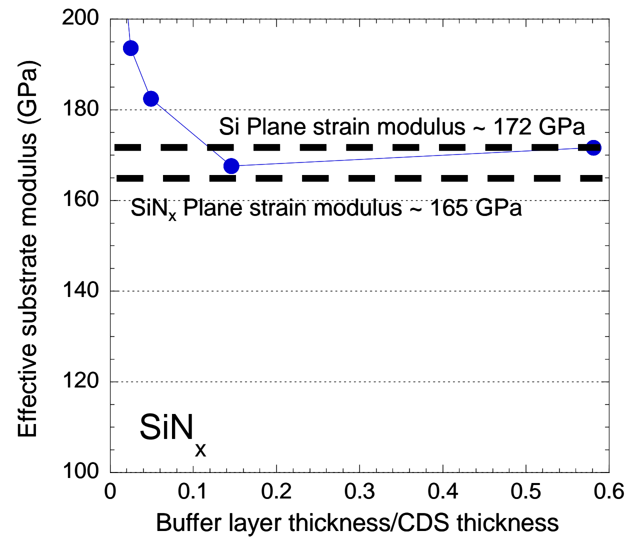

FIG. 4b. Effective substrate modulus of SiN_x buffer layer sample

This is followed by two materials – a spin-on organic polymer and low-density carbon-doped-oxide – that have elastic moduli that are approximately two times lower than the CDS modulus.

Crack velocity data for a 3.25 μm CDS film are plotted as a function of SiN_x and SiO_2 layer thickness in Fig. 3. The channel crack velocity for a CDS film of the same thickness deposited on bare silicon is labeled in the figure as a reference. The figure shows that channel cracks grow faster when CDS is deposited on buffer layers, than when deposited directly on Si. The composition, bond structure, residual stress, elastic modulus, and thickness of the CDS film do not depend on the buffer layer on which it is deposited. Consequently, the increased crack growth velocity can be attributed to the greater energy release rate applied to the CDS film as a result of the SiN_x and SiO_2 buffer layers. According to Eq. (1), the energy release rate for channel cracking in a film on a monolithic substrate is proportional to the elastic constraint factor, Z, which in turn is determined by the elastic modulus mismatch between film and substrate. If there is a buffer layer that is more compliant than the substrate, such as the SiN_x and SiO_2 layers in the current experiments, the constraint on the cracked film is reduced and the value of Z increases. The result is a larger energy release rate and crack propagation velocity as shown in Fig. 3. CDS films with a SiO_2 buffer layer have greater crack velocities than those with a SiN_x layer, because SiO_2 is more compliant than SiN_x (e.g., See Table 1). As the buffer layer thickness increases, the channel crack velocity approaches a limiting value that corresponds to the velocity of a channel crack in a CDS film deposited on a monolithic substrate made of buffer layer material. These limits are marked by the arrows in Fig. 3 and are in good agreement with the experimental measurements.

The constraint factor depends on the Dundurs parameters for both interfaces as well as on the buffer layer thickness. This effect can be presented through use of an "effective substrate modulus", which is calculated from experimental crack velocities. The effective substrate modulus is defined as the plane-strain modulus of a monolithic substrate that results in the same constraint factor as the system with the buffer layer. This effective stiffness depends on the buffer layer thickness and the elastic constants of the materials involved. In order to obtain a unique definition, the second Dundurs parameter β was taken equal to $\alpha/4$. Since the film stress

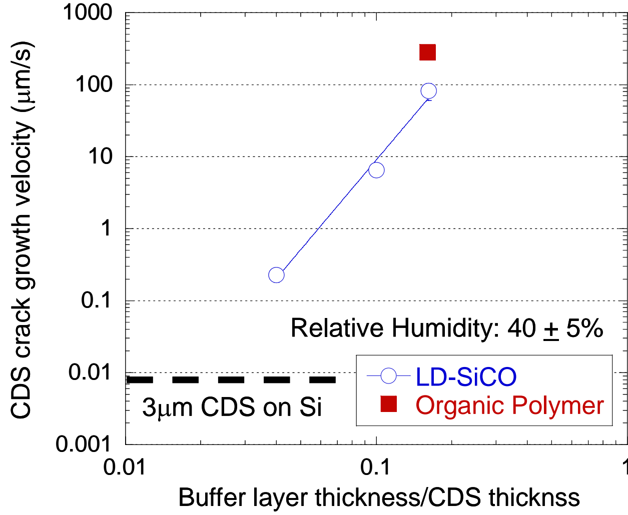

FIG. 5 Plot of CDS crack growth rate as a function of LD-CDO buffer layer thickness

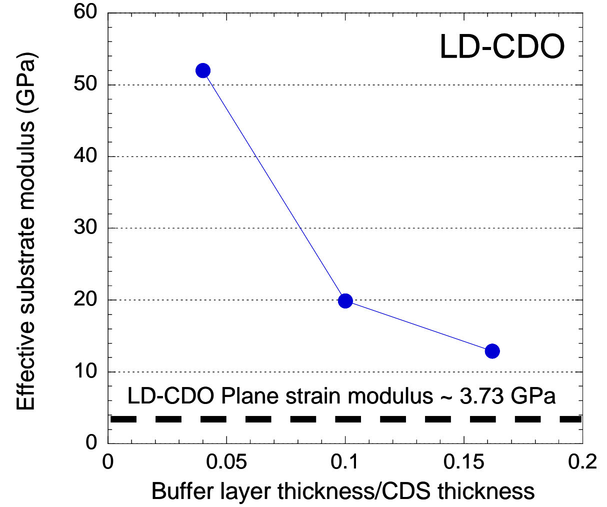

FIG. 6 Effective substrate modulus of LD-CDO buffer layer sample

and thickness are the same for all samples, the crack growth velocities in Fig. 3 can be converted to energy release rates using the data in Fig. 2. Using Equations (1) and (2) combined with the results in Fig. 1, these energy release rates are in turn converted to effective substrate moduli. Figures 4 (a) and (b) show the effective moduli for samples with SiO_2 and SiN_x buffer layers as a function of buffer layer thickness. For the SiO_2 layer, the effective modulus approaches the plane-strain modulus value for Si of 172 GPa, when the buffer layer is very thin, and the value for SiO_2 (75 GPa), when the buffer layer is thick. The trend for the SiN_x buffer layer is the same, but quantitative agreement is not quite as good. This is so because the value of the effective modulus for a compliant film on a stiff substrate depends sensitively on the precise value of α.

The constraint effect is much more dramatic when the CDS film is deposited on a more compliant low-density carbon doped oxide (LD-CDO) or the organic polymer buffer layer. Both of these materials have elastic modulus values of 3.5 GPa, which is smaller than the CDS modulus of 8 GPa, with a corresponding α value of 0.4. Figure 5 shows the channel crack velocity in a 3.0 μm CDS film as a function of the LD-CDO and polymer buffer layer thickness. Crack velocity increases rapidly with thickness and the rate of increase is significantly faster than for the samples with SiO_2 and SiN_x buffer layers shown in Fig. 3. With a 0.5 μm LD-CDO under-layer, the crack velocity is approximately four orders of magnitude larger than for CDS deposited on a bare silicon substrate with a value of approximately 100 μm/s. The effective substrate modulus for the LD-CDO buffer is plotted as a function of layer thickness in Fig. 6. The figure clearly shows that the effective modulus decreases very rapidly with buffer layer thickness and that it approaches the LD-CDO plane-strain modulus for buffer layer thicknesses as small as 0.5 μm.

It is useful to define a correction factor, M, to describe the effect of the buffer layer:

$$M = \frac{Z_{BL}\left(\alpha,\alpha_1,\beta_1,\beta_2,h_{BL}/h_f\right)}{Z_{Mono}\left(\alpha,\beta\right)} \approx \frac{Z_{BL}\left(\alpha,\alpha_1,h_{BL}/h_f\right)}{Z_{Mono}\left(\alpha\right)}, \tag{4}$$

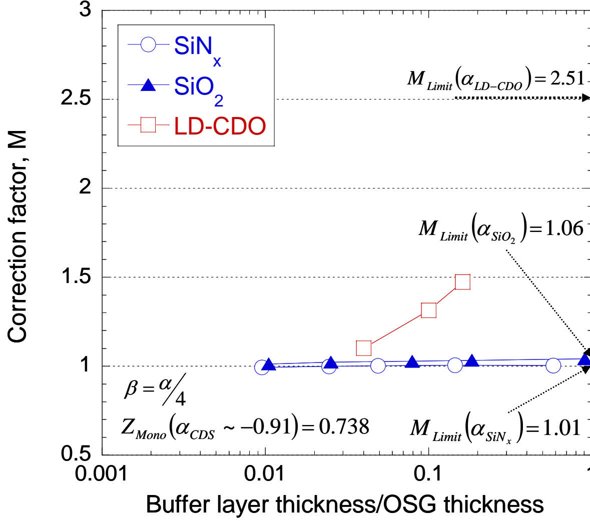

FIG. 7. Plot of correction factor (M) for as a function of buffer layer thickness.

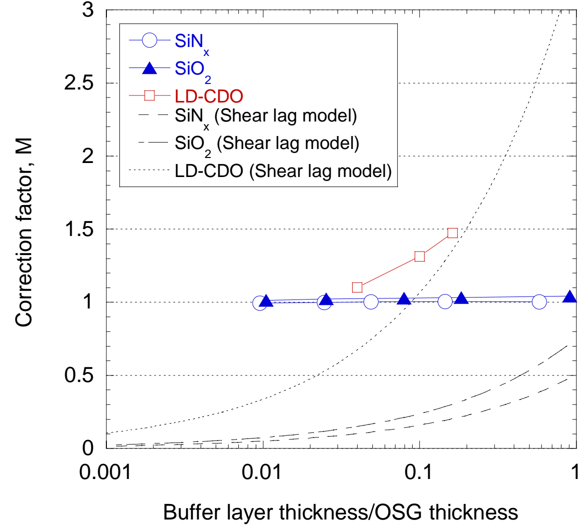

FIG. 8. Comparison of experimental data with shear-lag model.

where the subscripts BL and Mono refer to systems with a buffer layer and a monolithic substrate respectively. Subscript 1 refers to the CDS/buffer layer interface, and 2 to the buffer layer/substrate interface. Dundurs parameters without subscript refer to the CDS/substrate material couple. For simplicity, the functional dependence on β_1 and β_2 was neglected in Eq. (4). Figure 7 shows a compilation of the correction factors as a function of film thickness for all material systems considered in this study. For very small values of h_{BL}/h_f, the correction factor approaches unity, while for large values it approaches $Z_{Mono}(\alpha_1)/Z_{Mono}(\alpha)$. Suo [12-13] has proposed a simple shear lag model to calculate the driving force for channel cracking as a function of buffer layer thickness. According to this model, the energy release rate and the corresponding correction factor are given by

$$G=\sqrt{\frac{h_{BL}\bar{E}_f}{h_f\mu_{BL}}}\,\frac{\sigma^2 h_f}{\bar{E}_f}\quad\text{and}\quad M=\frac{1}{Z_{Mono}(\alpha)}\sqrt{\frac{h_{BL}\bar{E}_f}{h_f\mu_{BL}}}, \tag{5}$$

where μ_{BL} is the shear modulus of the buffer layer. The dashed lines in Fig. 8 represent the correction factors for the various buffer layers according to Eq. (5). Agreement with experimental results is fairly poor even for the most compliant buffer layer. This is so because Eq. (5) only considers the effect of the buffer layer, and neglects the contribution of the substrate. As a result, the formula predicts a vanishing energy release rate in the limit of zero buffer layer thickness. In the limit when the buffer layer thickness approaches infinity, the energy release rate grows without bound, which is also unrealistic.

The crack propagation rate results discussed above demonstrated that a compliant buffer layer can significantly alter the cracking behavior by reducing elastic constraint from the silicon substrate. It is instructive to investigate how back-end-of-line (BEOL) multilayered structures

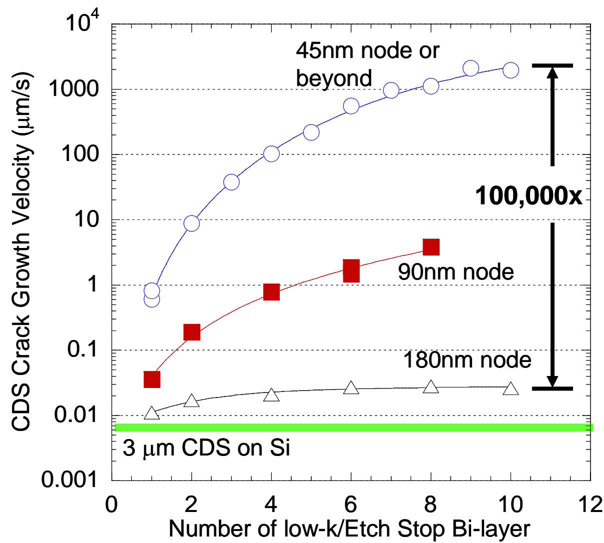

FIG. 9. CDS crack growth velocity as a function of low-k/etch stop layers.

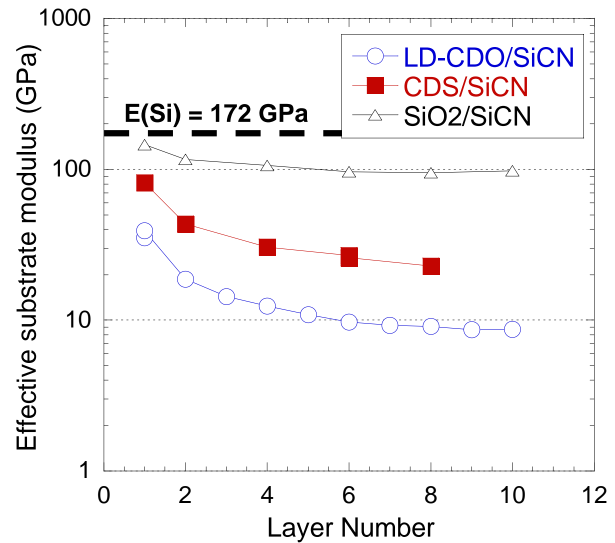

FIG. 10. Effective substrate modulus values as a function of layer number.

that consist of alternating layers of a low-k dielectric and a stiff etch-stop material affect the elastic constraint and crack growth rate. In this part of the study, samples deposited with one to ten bi-layers comprising a 300 nm low-k dielectric and a 60 nm silicon carbo-nitride (SiCN) etch-stop were prepared. The elastic modulus of SiCN is 100 GPa and the film has a residual compressive stress of 275 $\pm$ 10 MPa. Three different bi-layer systems with different low-k materials were prepared representing three generations of BEOL technology nodes – SiO_2 (130 nm node), CDS (90 nm), and LD-CDO (45 nm and beyond). All bi-layer samples were capped with 3 μm thick tensile CDS films. The CDS channel crack propagation rates are plotted in Fig. 9 as a function of the number of bi-layers deposited beneath the CDS films. The figure shows that crack velocities for the three dielectric systems increase rapidly for the initial three bi-layers and begin to plateau for greater numbers of bi-layers. This indicates that the elastic constraint reduction is greatest for the first three layers of materials. A reduction in elastic constraint is indeed expected as all of the bi-layer materials have smaller elastic modulus values than the silicon substrate. It is important to note that, at the tenth low-k/etch stop layer, the crack propagation rate in the LD-CDO/SiCN system (45 nm node) is approximately five orders of magnitude faster than its SiO_2/SiCN (130 nm node) counterpart. These data indicate that channel cracking will be a significant challenge for the integration of future 45 nm technology node devices. The effective substrate modulus values of the three multilayered systems are plotted as a function bi-layer number in Fig. 10. The figure shows that the effective modulus values converge to that of the silicon substrate value at 172 GPa when the number of low-k/etch-stop layers is reduced. As the number of layers increases, the effective moduli approach the intrinsic values of the corresponding low-k dielectric.

CONCLUSIONS

It has been demonstrated that the subcritical channel crack growth rate in carbon-doped silicate (CDS) coatings depends sensitively on the elastic properties and thickness of underlying layers. An underlying layer that is more compliant than the substrate results in an increase of the

energy release rate and a corresponding increase in crack velocity. If the underlying layer is stiffer, the energy release rate is reduced and so is the crack velocity. The effect of the underlying layer on the channel cracking energy release rate increases with the thickness of that layer and can be described by means of a simple correction factor in the expression for the energy release rate. The correction factor depends on the Dundurs parameters of the interfaces involved and on the thickness of the underlying layer. These observations have important implications for the reliability of brittle coatings: In addition to the residual stress, thickness, and fracture toughness of a coating, one also needs to consider the precise film stack to determine whether the coating is prone to channel cracking.

REFERENCES

1. Q. Ma, “A Four-Point Bending Technique for Studying Subcritical Crack Growth in Thin Films and at Interfaces”, J. Mat. Res., **12**, 840-845 (1997)
2. M. Lane, N. Krishna, I. Hashim, and R. H. Dauskardt, “Adhesion and Reliability of Copper Interconnects with Ta and TaN Barrier Layers”, J. Mat. Res., **15** [1] 203-211, (2000)
3. Ting Y. Tsui, A. J. Griffin, Jr., Jeannette Jacques, Russell Fields, Andrew J. McKerrow, and Robert Kraft, “Effects of Elastic Modulus on the Fracture Behavior of Low-Dielectric Constant Films”, Proceedings of the 2005 IEEE International Interconnect Technology Conference, IEEE Electronic Devices Society, Burlingame, California, June 2005.
4. A.A. Volinsky, P. Waters, J.D. Kiely, E. Johns, “Sub-Critical Telephone Cord Delamination Propagation”, Mat. Res. Soc. Symp. Proc. Vol. 854E, U9.5 (2004)
5. J.J. Vlassak, “Channel cracking in thin films on substrates of finite thickness”, International Journal of Fracture **119** (4), 299-312 (2003)
6. R.F. Cook and E.G. Liniger, “Stress-corrosion cracking of low-dielectric-constant spin-on-glass thin films”, Journal of the Electrochemical Society, **146**, 4439-48 (1999)
7. J.L. Beuth Jr., “Cracking of thin bonded films in residual tension”, International Journal of Solids and Structures, **29**, 1657-75 (1992)
8. Dundurs J. “Edge-bonded dissimilar orthogonal elastic wedges”, J. Appl. Mech., **36**, 650-652 (1969)
9. B.R. Lawn, Fracture of Brittle Solids, 2nd ed. (Cambridge Press, Cambridge, 1993).
10. S. M. Wiederhorn and H. Johnson, “Effect of Electrolyte pH on Crack Propagation in Glass”, Journal of The American Ceramic Society, **56** (4), 192 (1973).
11. T. H. Courtney, Mechanical Behavior of Materials, (McGraw-Hill Publishing Company, 1990).
12. Z. Suo, “Reliability of interconnect structures”, in Comprehensive Structural Integrity, Vol 8, Interfacial and Nanoscale Fracture, p 265-324, edited by I. Milne, R.O. Ritchie, and B. Karihaloo (Elsevier, 2003)
13. Jun He, Guanghai Xu, and Z. Suo, “Experimental Determination of Crack Driving Forces in Integrated Structures”, Proceedings of the 7th International Workshop on Stress-Induced Phenomena in Metallization, Austin, Texas, edited by P.SW. Ho, S.P. Baker, T. Nakamura, C.A. Volkert, American Institute of Physics, New York, pp 3-14, June 2004.